Nanotechnology Perceptions
ISSN 1660-6795
www.nano-ntp.com

Role Of Zncro4 and Graphene Mixture in Boosting Corrosion Resistance of Mild Steel

Dhivya Christo Anitha S[1], Mary Jenila R[2*]

[1]Research Scholar Department of Physics, St. Xavier's College, Palayamkottai -627002 Manonmaniam Sundaranar University, Tirunelveli, Tamilnadu, India
[2]Assistant Professor Department of Physics, St. Xavier's College, Palayamkottai-627002Manonmaniam Sundaranar University, Tirunelveli, Tamilnadu, India
Email: jenilasimon@gmail.com

In the present work, graphene has been added with ZnCrO4 solution in mild steel to mitigate the metal corrosion. Graphene in the concentrations of 1, 2 and 3% were mixed with ZnCrO4 paint. Studies such as FT-IR, SEM, EDAX, AC impedance, cyclic voltammetry, and Tafel analysis were used to examine the physical properties of the materials. The inhibitory efficiency was measured using the weight loss method. The functional groups present in the material was examined using FT-IR spectroscopy. The morphology and shape behaviour of the prepared specimens was evaluated by scanning electron microscopy. The elemental composition of the specimen was determined using EDAX. The corrosion current density and linear polarisation resistance were calculated using Tafel analysis. AC impedance and cyclic voltammetry provide information on the protective layer that is created on the specimen to prevent corrosion. From the studies, it is understood that, graphene significantly enhances the corrosion resistance properties of mild steel.
Keywords: Mild steel, Corrosion resistance, ZnCrO4 and Graphene.

1. Introduction

Mild steel is employed in vast range of industries because of its accessibility along with economic and promising mechanical characteristics [1]. Generally, in the chemical industries, acid solutions are widely utilised for the purpose of acid pickling and cleaning. However, due to the weak corrosion resistance properties of mild steel towards acids, enhancing the corrosion stability in acidic environment is need of the hour[2–4]. Also, it is to be noted that, rust never runs out. Retrieving the metals from stable ores such as oxides, sulphides and carbonates requires a significant amount of energy. When a metal reacts with

its environment, it corrodes, eroding the substance or its properties[5]. In particular, if significant attention is not given, mild steel may get corroded more easily compared to pristine alloys like stainless steel due to the existence of minute alloying particles[6]. Researchers havebeen givingmore emphasis on controlling corrosion than preventing it because corrosion cannot be eliminated. Increase in humidity levels and salinity make the mild steel to deteriorate heavily in the harsh environments paving way for massive economic loss and health concerns [7]. Usually adopted cost effective techniques for corrosion prevention includes barrier coating which involves painting, plastics and powder etc[8]. A thin layer can be formed on the metal surface if powders such as epoxy, nylon and urethane are employed. It is to be noted that, metal surfaces are some sometimes sprayed by plastic and waxes. Paint can act as a protecting layer that can shield the metal surface from electrochemical reactions caused by corrosive chemicals[9]. In today's technological advancement, the paints are created with multiple layers of paint which can perform various tasks. The priming coat functions as an inhibitor, the intermediate coat thickens the paint, and the final coat protects it from the other elements[10].

Mild steel is used in most of building sectors due to its ability to be strong. Excellent flexibility of the mild steel when utilized in steel framing is another key characteristic[11]. Buildings made of mild steel also deteriorate due to environmental factors. In order to prevent these difficulties, steel is frequently coated with zinc chromate to prevent corrosion[12]. However, the zinc chromate primer is quite toxic and also gets rid of organic development on steel surfaces[13]. This leads to its use in the creation of linoleum, artist's paints, varnish pigments, and spray paints. A new era of cutting-edge materials is expected to begin with the two-dimensional substance graphene, which has a single layer and a thickness of just one atom diameter (about 0.35 nm)[14]. The strong barrier performance, good mechanical characteristics, and noticeable aspect ratio of graphene, makes it possible for a route from the corrosive media to the metal substrate can be greatly lengthened[15]. As a consequence of this, fields such as anti-corrosion coatings and metal surface treatment have seen the influence of graphene [16]. The best shielding properties and single-layer graphene without any flaws are found in the thinnest corrosion-prevention covering. The greatest anti-corrosion coating will eventually be made of graphene because of its exceptional thermal, electrical, and mechanical properties [9, 10].Because of its surface area and small particle size, graphene functions as a reliable barrier between metal and oxygen[17]. Graphene additionally strengthens the surface bond between the covering and the metal substrate. These elements work as a unit to prevent any water vapor from reaching the metal. Graphene is being employed in the mission to improve the zinc chromate primer paint's ability to prevent corrosion[18]. Traditional organic coatings include the risk of heavy metals like lead which is a threat to human society. It's incredibly detrimental to the long-term development of society and the economy, as well as consuming a lot of non-renewable energy [19]. To best of our knowledge, there are hardly few reports that have worked on utilizing graphene in $ZnCrO_4$ for enhancing the corrosion resistance properties. In the present work, graphene has been added with $ZnCrO_4$ solution in amounts of 1, 2 and 3% and the physical properties of mild steel has been systematically evaluated.

2. Materials and Methods

All the reagents used in the present work are of analytical grade with 99% purity. Mild steel having a composition (wt %) of C=0.17, Mn=0.46, Si = 0.26, S = 0.017, P = 0.019, and balance Fe was used. Graphene was purchased from Ad Nanotechnologies Pvt. Ltd. It is produced from chemical exfoliation methods with multiple points of quality checks. According to the data given by the company its thickness is 5-10 nm and having surface area of 60-200 m^2/g and $ZnCrO_4$ paint primer.

2.1 Preparation of the Specimen

Figure 1 displays the schematic representation of coating process. Specimens of mild steel having dimensions of (1.9 cm* 4.3 cm * 0.4 cm) was cleaned and polished with emery paper. After that it was washed with acetone followed with deionized water and then dried at a temperature of 120°C using an oven. Before coating, the weight of mild steel was noted. Zinc chromate primer solution was stirred for1 hour duration. Separately, in another beaker, graphene solution was added with few drops of 1 propenal and stirred for 1 hour. Later, the two solutions were mixed together and again stirred for 1 hour. Using dip coating method, the steel plates were coated with solutions of zinc chromate primer of 100cc mixed with graphene concentrations ranged from 1%, 2%, and 3%. Then it was dried in an oven at 120^0C for three hours. These coated mild steel specimens were subjected to bore water treatment for 10 days. After that samples were weighed and subject to various characterizations to investigate the physical properties of mild steel.For convention, the mild steel without any coating is named as metal, mild steel with $ZnCrO_4$coating is named as Zn, mild steel with $ZnCrO_4$ and graphene 1,2 and 3% concentration coating are named as Zn+G1%, Zn+G2% and Zn+G3% respectively.

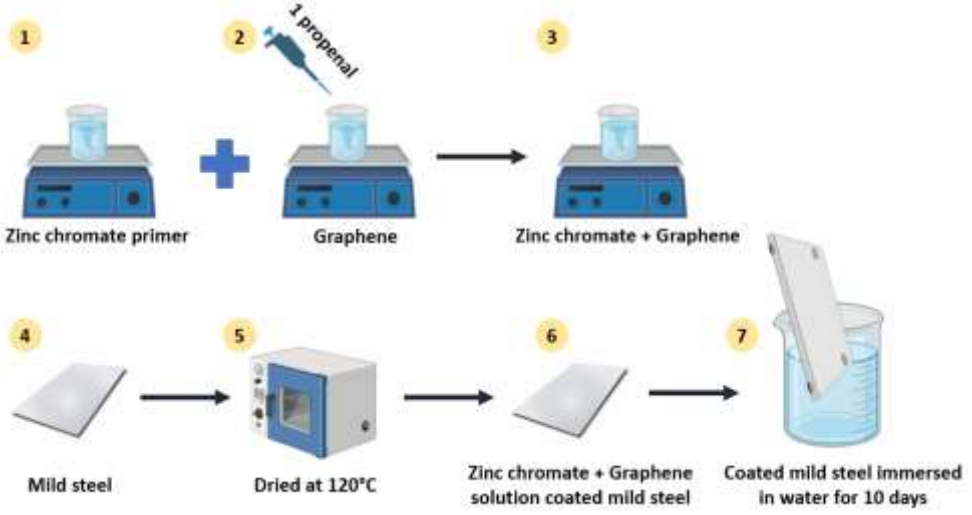

Figure 1: Schematic representation of coating process

2.2 Materials Characterization

The Tafel analysis was performed using an Ag/AgCl electrode as reference and Platinum

wire as counter electrode. AC impedance spectra weremeasured using Versa STAT MC in the Frequencyrange 1Hz to 1MHz at room temperature. The weight loss method was performed by Nivayo digital weight machine(500g capacity and 0.01 g accuracy). For the weight loss method, the samples were initially coated with $ZnCrO_4$ and graphene solution and weighed (W1). After that, the samples were immersed in bore water for a period of 10 days and remeasured again (W2). The FT-IR spectra of the samples were performed using Perkin Elmer spectrometer in the range 400-4000 cm^{-1}. The morphology and shape behavior of the samples were performed using Carelzeiss, Evo 18 scanning electron microscope. The elemental composition was determined using Tescan Oxford INCA detector. The cyclic voltammetrystudies of the samples were performed usingVersa STAT MC in the potential range of -2mV to 2mV at room temperature.

3. Results and Discussions

3.1 Tafel Analysis

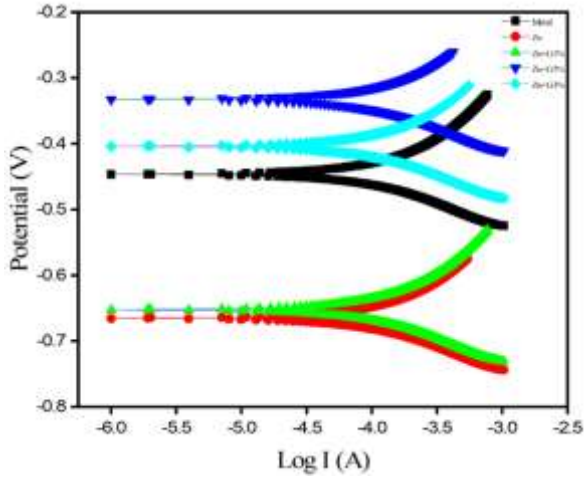

Figure 2: Tafel analysis of uncoated and coated mild steel with $ZnCrO_4$ and Graphene coating

Table 1- Corrosion parameters of uncoated and coated mild steel from tafel

Inhibitor	E_{corr}	β_c	β_a	I_{corr}	LPR	IE%
Metal	-446.52	0.0292	0.0168	-3.8672	167.08	-
Zn	-658.328	91.639	117.74	26.288	352.29	86.83
Zn+G1%	-658.935	124.351	266.674	81.627	451.713	89.11
Zn+G2%	-317.479	276.813	244.878	5.531	1063.89	97.2
Zn+G3%	-420.71	115.483	131.687	5.731	4667.59	97.3

The Tafel analysis was employed to understand the corrosion phenomenon of mild steel with and without coating. Figure 2 displays the potentiodynamicpolarisation curves for each sample. The relationship between the overpotential and lograthimic current density can be clearly seen from the Tafel's plot. By adopting the extrapolation approach, some important parameters such as Tafel's slope, corrosion current density and corrosion potential can be evaluated[20]. A corrosion potential value of -446.52 mV was obtained for mild steel

without coating. Interestingly, the corrosion potential was seen to change when mild steel was treated with zinc chromate with different amounts of graphene. For $ZnCrO_4$, the value seems to be around -658.328mV which experiences a slight change in the decimal units after the addition of graphene 1%. Furthermore, the value raises up to -317.479 mV for 2% of graphene and again drops to -420.71 mV for graphene 3%. Additionally, the linear polarization resistance curve is seen to increase while the corrosion potential curve decreases. When compared to mild steel without a coating, mild steel with a graphene coating has a high LPR value. Similarly, the inhibition efficiency which is expressed by IE% in the table 1 is found to be around 86.83 for $ZnCrO_4$ which experiences a drastic increase up to 97.3 for $ZnCrO_4$+G3%. According to this, the coating layer serves as a shield to prevent corrosion on the metal surface. In order to prevent corrosion, graphene's thick coating acts as a barrier.

3.2 AC Impedance Spectra

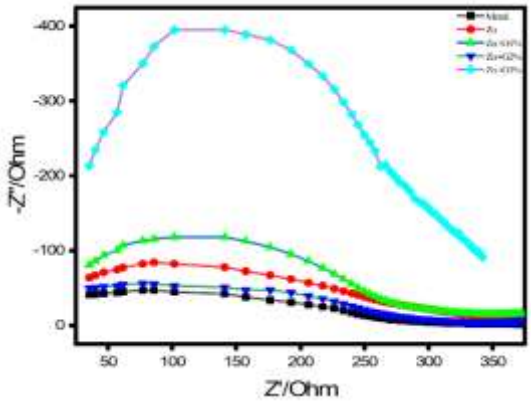

Figure 3: AC impedance spectra of Nyquist plot for uncoated and coated mild steel

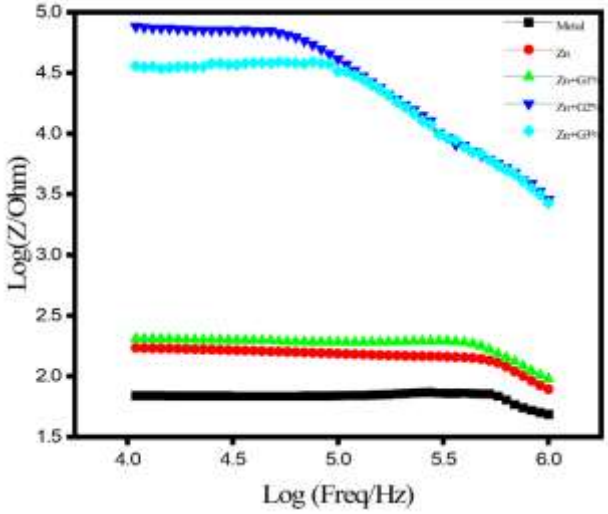

Figure 4: Impedance Bode plot

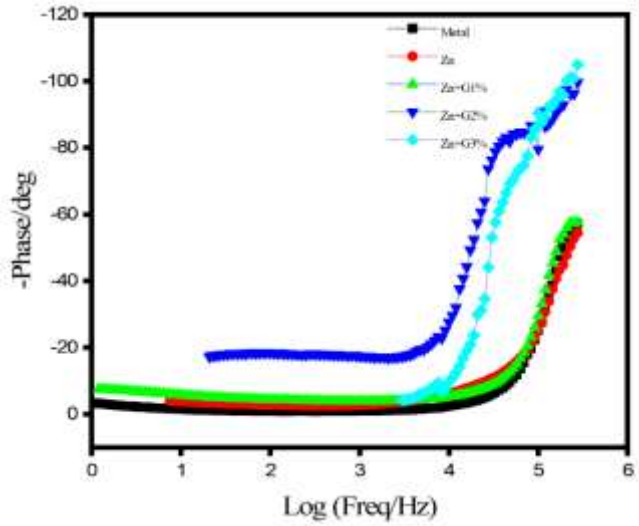

Figure 5: Phase bode plot

The rate of change of corrosion properties of metals protected by a thin electrolyte layer was determined by impedance spectroscopy[21]. Figures 2-4 display the Nyquist plot, impedance bode plot, and phase bode plot of coated and uncoated mild steel. It has been demonstrated through the use of Ac impedance spectra that a protective layer has developed on the metal surface [22]. An increase in charge transfer Sis also observed. A higher value of R suggests the integrity of the coating system, which also signifies that corrosion reactions under coatings would progress more slowly. It is to be noted that, double-layer capacitance is seen to be declining, while charge transfer resistance and impedance bode plot values are rising. The observed phenomenon illustrates that, the mild steel will have a barrier against corrosion provided by the coating layer. Table 4 below displays the R_c and C_{dl}values for uncoated and coated mild steel.

Table 2- Corrosion parameters of uncoated and coated mild steel from impedance data

Inhibitor	R_c	C_{dl}	Bode plot	IE%
-	50.0665	$1.01x10^{-7}$	1.88	-
$ZnCrO_4$	162.6357	$3.13x10^{-8}$	2.31	69.21
Zn+G1%	168.416	$3.01x10^{-8}$	2.37	70.27
Zn+G2%	234.628	$2.17x10^{-8}$	2.45	78.6
Zn+G3%	352.170	$1.44x10^{-8}$	4.55	85.78

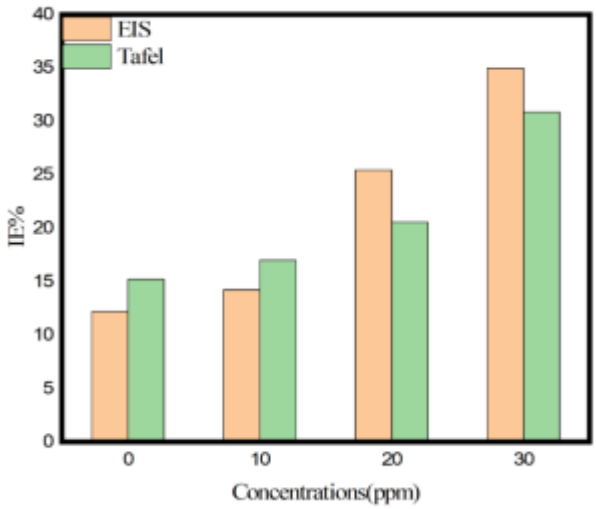

Figure 6: IE% for both Tafel and impedance measurements

3.3 Adsorption Isotherm

Adsorption of inhibitors rarely reaches real equilibrium on corroding surfaces, but rather has a tendency to stabilize. In the presence of an inhibitor, the adsorption steady state leads to a quasi-equilibrium state when the corrosion rate is significantly decreased. Furthermore, by using adequate adsorption isotherm, the trend of quasi equilibrium inhibitor adsorption can be investigated. Surface coverage area, concentrations of the inhibitor, and equilibrium constant for the adsorption/desorption process make up the Langmuir adsorption isotherm.

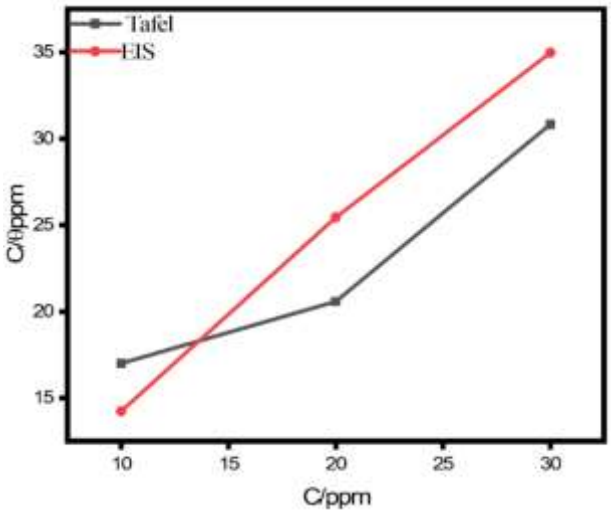

Figure 7: Langumir adsorption isotherms for mild steel coated with various concentrations of Graphene using EIS and Tafel

The free energy of adsorption, ΔG°adscan be expressed as:

$$\triangle G^{0}_{ads} = -RTln(55.5K_{ads}) \quad (1)$$

where T is the absolute temperature and the constant value of 55.55 is the molar concentration of water. The spontaneity of the adsorption process and the stability of the adsorbed coating on the mild steel surface are both guaranteed by the negative values of $G°_{ads.}$ It is generally agreed that values of $G°_{ads}$ around -20 kJ mol^{-1} or lower represent the electrostatic interaction of charged organic molecules and metal surfaces in the majority of the solution (physisorption process), while values of $G°_{ads}$ around -40 kJ mol^{-1} or higher represent the charge sharing or transfer of charged metal surfaces to organic molecules (chemisorption process). The table shows the calculated values for G_{ads} and K_{ads}[23].

Table 3- Thermodynamic adsorption parameters

Inhibitors	$-\Delta G^0$/KJ mol^{-1}		K_{ads} ($x10^3$ mol^{-1})	
	Tafel	EIS	Tafel	EIS
$ZnCrO_4G$	14.393	13.741	5.468	4.212

3.4 Weight-Loss Method Analysis

To determine weight loss in this experiment, the weight of each sample was measured both before and after ten days of complete immersion in the medium. The weight loss that was used to determine mild steel's inhibitory efficiency was measured using the difference between the initial and final weights. The following formula was used to compute the inhibition efficiency, is given by the following equation,

$$IE = 100\left(1 - \frac{W_1}{W_2}\right) \quad (2)$$

Where, W_1- refers to weight before the immersion and W_2 refers to weight after the immersion

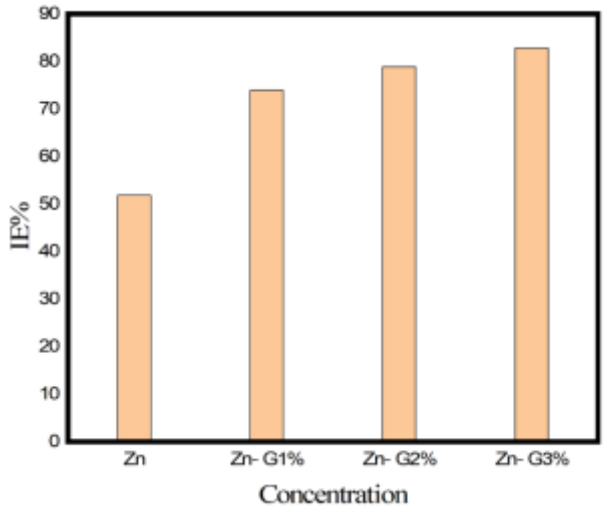

Figure 8: Inhibition efficiencies of mild steel from weight loss method

Figure 8 displays the $ZnCrO_4$-Graphene-coated inhibitory effectiveness. It has been

identified that inhibiting effectiveness increases along with the concentration of graphene. The protective layer that has developed to prevent corrosion on the metal surface is the main cause of this result. The efficiency of the zinc chromate primer is increased when graphene is added to it. The corrosion barrier is strengthened with graphene.

3.5 Analysis of FT-IR Spectra

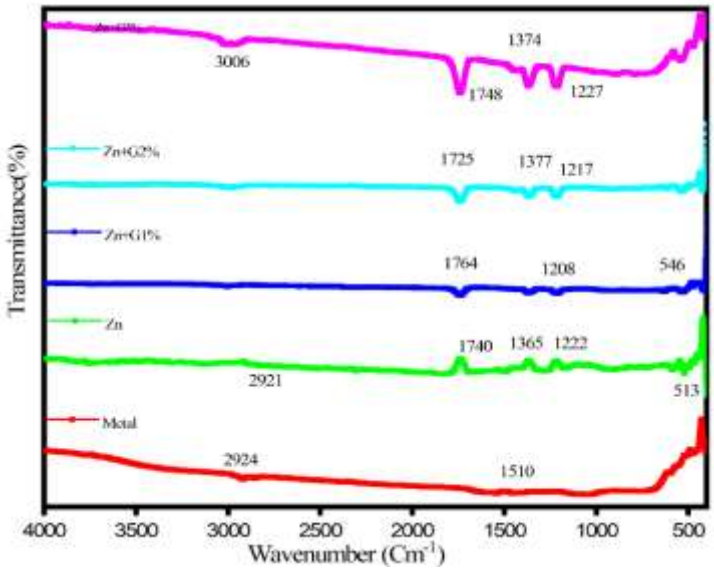

Figure 9: FTIR Spectra of uncoated and coated mild steel of zinc chromate with Graphene coating

FT-IR spectroscopy is a quantitative tool for analysing functional groups and obtaining information on covalent bonding. Figure 9 displays the FT-IR spectra of both coated and untreated mild steel. In case of pure metal, no peaks related to $ZnCrO_4$ or graphene is observed. However, upon addition of $ZnCrO_4$, an adsorption layer forms as a result of a higher tendency for the organic coating to donate π-electrons to the appropriate empty d-orbital of the steel. Inhibitors with bond electrons have superior anticorrosive properties. In $ZnCrO_4$, the peak at 3743cm^{-1} is associated with O-H stretching vibration due to the alcohol groups. The strong and broad peak at 2921cm^{-1} is identified as the C-H stretching vibration of alkane groups. The peak at 1740cm^{-1} is the strong and broad peak of C=O stretching vibration. The O-H bending vibration is identified by the peak at 1365cm^{-1}. The C-O stretching vibration is associated with the peak at 1232 cm^{-1}. In Zn+G1%, the strong and broad peak at 3037cm^{-1} is related to the O-H stretching of water. The peak 1740cm^{-1} is the C=O stretching vibration of aldehyde groups. The strong peak of C-O stretching vibration is identified at 1280 cm^{-1}. In Zn+G2%, the strong broad peak at 3538cm^{-1} is associated with the water molecules. The medium peak at 2917cm^{-1} is refereed C-H stretching vibration. The peak at 1725$cm^{-1}$and 1075cm^{-1} is associated with C=O stretching and C-O stretching vibration. In Zn+G3%, the strong and broad peak of O-H stretching is identified at 3014cm^{-1}. The peaks 1716 cm^{-1} and 1374$cm^{-1}$are referred C=O stretching and O-H bending vibration group and the strong peak at 1227 cm^{-1} is related to the C-O stretching

vibration.

3.6 SEM & EDAX

A visual representation of mild steel with and without coating is illustrated through SEM images in Figure 10(a–e). From the image, it is identified that, the object seems to be deteriorated, by the mild steel without a coating with 20 m magnification. The absence of an inhibitor could have caused the surface to corrode. After the steel was coated with graphene, there seemsto be no deterioration. This phenomenon may be due to the specimen being protected by the graphene layer. The enormous surface area of graphene makes it possible to blend. Sulfation corrosion is negligible without graphene. There is no corrosion, and a graphene coating made the surface incredibly smooth. Mild steel is protected against corrosion by the protective graphene covering.

The elemental compositions present in the prepared materials have been investigated using EDAX spectroscopy. Figure 10 displays the EDAX spectrum of uncoated and mild steel. Fe, carbon, and oxygen together account up 50.75 percent of the surface of mild steel. Steel with a $ZnCrO_4$ coating comprises 42.49 %Fe, and 51.42 % oxygen. The proportion of Fe and oxygen atoms in the $ZnCrO_4$drops when graphene is added. The percentage of Fe and oxygen in $ZnCrO_4$ by atomic weight falls as graphene material is gradually added. This indicates that, as graphene is added, Fe content decreases suggesting that graphene may act as a protective layer thereby restricting the percentage of corrosion.

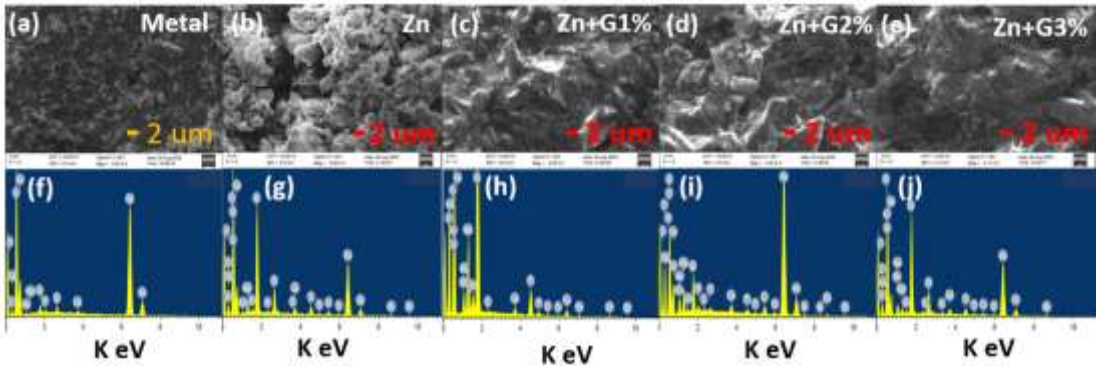

Figure 10: (a-j) SEM images& EDAX spectrum of a) Metal, b) Zn, c) Zn+G1%, d) Zn+G2%, e) Zn+G3%

Table 4 below shows the proportion of Fe and oxygen by atomic weight for mild steel and coated steel.

Table 4 Atomic weight percentage of elements in the uncoated and coated mild steel

Inhibitor	Fe %	O %
Metal	50.75	42.44
Zn	42.49	51.42
Zn+G1%	37.09	47.17
Zn+G2%	21.73	43.18
Zn+G3%	0.98	25.44

3.7 Cyclic Voltammetry

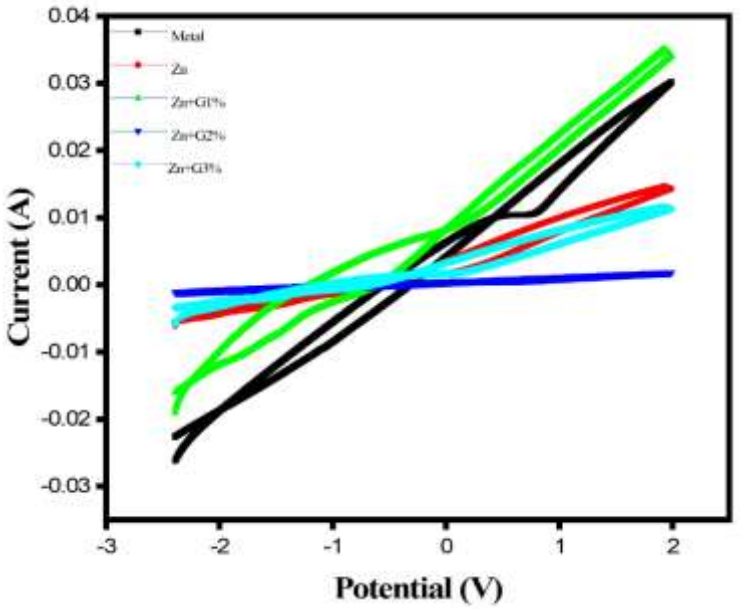

Figure 11: Cyclic Voltammogram of uncoated and coated mild steel

Cyclic voltammetry, an electrochemical method, measures the current that develops in an electrochemical cell when the voltage exceeds what the Nernst equation predicts. The electrochemical band gap value and HOMO–LUMO energy levels were determined using cyclic voltammetry. The following formula can be used to determine the compound's HOMO–LUMO energy levels based on the electrochemical data.

$$\mathrm{HOMO} = -[4.65\mathrm{V} - \mathrm{E_{OX}(onset)}] \quad (3)$$

$$\mathrm{LUMO} = -[4.64\mathrm{V} - \mathrm{E_{Red}(onset)}] \quad (4)$$

The Lowest Unoccupied Molecular Orbital (LUMO) and Highest Occupied Molecular Orbital (HOMO) to better understand the chemical stability of the doped graphene. Some information about the chemical stability can be obtained from the HOMO-LUMO gap. To assess the reactivity of inhibitor compounds, the energy of the lowest unoccupied molecular orbital (ELUMO), the highest occupied molecular orbital (EHOMO), and global reactivity characteristics including chemical hardness (η), chemical potential (μ), and electrophilicity index (ω) were derived. According to Parr (1989), chemical potential is the opposite of electronegativity. The ability of an electron or a collection of atoms to draw other electrons towards them is measured by their electronegativity.

$$\mu = \chi \quad (5)$$

Koopman's theorem, about the energy of HOMO and LUMO, was used to determine the molecular properties of inhibitors that correspond to their reactivity and selectivity. These characteristics include ionization potential (I), electron affinity (A), electronegativity (χ), global hardness (η), and softness (σ). The amount of energy needed to extract an electron from a molecule is known as the ionization potential. The easier it is to extract an electron

from a molecule, the lower the ionization potential. A high ionization energy is indicative of chemical inertness and stability, whereas a lower ionizationenergy is indicative of strong atom and molecular reactivity. The equation can be used to connect the ionization potential (I) to the energy of the E_{HOMO}.

$$I = -E_{HOMO} \quad (6)$$

Using the following equation, electron affinity (A) and ELUMO can be connected

$$A = -E_{LUMO} \quad (7)$$

Between the values of I and A, one can figure out electronegativity (χ) and global hardness (η). The core definition of chemical hardness is the ability to withstand tiny perturbations in a chemical reaction, such as deformation or polarisation of the electrocloud of atoms, ions, or molecules. The tendency for a soft molecule to respond is higher than that of a hard molecule. An energy gap is larger in hard molecules and less in soft molecules.

The inhibitor molecule's absolute electronegativity (χ) and chemical hardness (η) can be expressed as follows:

$$\chi = ((I + A))/2 \quad (8)$$

$$\chi = ((I - A))/2 \quad (9)$$

The tendency of an atom or group of atoms to receive electrons is measured by electron polarizability, or σ. This was determined using the following equation:

$$\sigma = 1/2\eta \quad (10)$$

Values for electrophilicity indicate whether a molecule is nucleophilic or electrophilic. A high electrophilic value indicates an increased tendency for the molecule to behave as an electrotrophile, whereas a low electrophilicity value indicates a high propensity for the molecule to act as a nucleophile.

$$\omega = \mu^2/2\eta \quad (21)$$

The above formulacan be used to determine the absolute electrophilicity index.The HOMO energy signifies a graphene molecule's desire to share an electron since it correlates to the ionisation potential. While the LUMO energy is a measure of the electron transport level and correlates with the electron affinity, a higher HOMO energy may indicate an increased ability to donate electrons. An inhibitor molecule has a stronger propensity to take electrons when its LUMO energy is lower.Published research [24] suggests the main factor influencing the prediction of the chemical reactivity and stability of inhibitor compounds is the energy gap, or ΔE. An inhibitor molecule gets more reactive when its value of ΔE decreases. A molecule's ability to avoid corrosion is increased by a higher HOMO energy. Conversely, a molecule's LUMO energy (ELUMO) value indicates its propensity to take on an electron from a metal atom. A decrease in (ELUMO) indicates a molecule's capacity to take up an electron from a metal atom. As a result, a molecule's corrosion inhibition efficiency rises with decreasing LUMO energy which is shown in table 5.

Table 5 Chemical parameters of the uncoated and coated mild steel

Inhibitor	E_{homo} (eV)	E_{Lumo} (eV)	ΔE_{gap}	Ionization potential(I)	Electron affinity(A)	Electron negativity(χ)	Global hardness(η)	Chemical potential(μ)	Chemical softness(σ)	Global electrophilicity(ω)
Metal	-4.673	-4.963	-0.29	4.673	4.963	4.818	-0.145	-4.818	-0.0725	78.8
$ZnCrO_4$	-4.8051	-5.0818	-0.276	4.8051	5.0818	4.9434	-0.1383	-4.9434	-0.06915	-1.689
$ZnCrO_4G1$	-4.5156	-5.0487	-0.583	4.5156	5.0487	4.7821	-0.2665	-4.7821	-0.13325	-3.0472
$ZnCrO_4G2$	-4.646	-5.2769	-0.63	4.646	5.2769	4.961	-0.6309	-4.961	-0.31545	-7.763
$ZnCrO_4G3$	-4.7653	-5.63	-0.86	4.7653	5.63	5.196	-0.4323	-5.196	-0.21615	-31.22

4 Conclusion

Zinc chromate and graphene have been combined in various quantities and coated on the steel. To determine the rate of corrosion, mild steel was dipped into bore water after the coating had dried. The functional group of the graphene bonding vibrations is confirmed by the FTIR spectra. The morphology of the mild steel was examined using SEM. The steel that was not coated was covered in rust. In order to prevent corrosion in the coated mild steel, graphene created a barrier. The element present in the samples was assessed by the EDAX. The low proportion of Fe atoms in zinc chromate paint mixed with graphene shows that the corrosion rate is low when the graphene serves as a barrier.Cyclic voltammetry and AC impedance are used to show that the steel has been wrapped in a layer of graphene to prevent corrosion. The corrosion current density and linear polarisation resistance were calculated using Tafel analysis. When the corrosion current density decreases, the LPR value rises.

Competing interests

The authors declare that they have no known competing financial interests or personal relationships that could have appeared to influence the work reported in this paper.

Research Data Policy

The data will be available on reasonable request mode

Conflict of interest

There is no conflict of interest

References

[1] Y. Li, P. Zhao, Q. Liang, B. Hou, Berberine as a natural source inhibitor for mild steel in 1M H2SO4, Applied Surface Science 252 (2005) 1245–1253. https://doi.org/10.1016/j.apsusc.2005.02.094.

[2] S. Banerjee, V. Srivastava, M.M. Singh, Chemically modified natural polysaccharide as green corrosion inhibitor for mild steel in acidic medium, Corrosion Science 59 (2012) 35–41. https://doi.org/10.1016/j.corsci.2012.02.009.

[3] I. Ahamad, R. Prasad, M.A. Quraishi, Inhibition of mild steel corrosion in acid solution by Pheniramine drug: Experimental and theoretical study, Corrosion Science 52 (2010) 3033–3041. https://doi.org/10.1016/j.corsci.2010.05.022.

[4] W. Li, M. Mase, T. Inui, M. Shimoda, K. Isomura, H. Oda, K. Yamada, Y. Urade,

Pharmacokinetics of recombinant human lipocalin-type prostaglandin D synthase/β-trace in canine, Neuroscience Research 61 (2008) 289–293. https://doi.org/10.1016/j.neures.2008.03.006.

[5] O.D. Ogunleye, O.A. Odulanmi, O.S.I. Fayomi, Corrosion Characteristics and Passive Behavioral Responses, IOP Conf. Ser.: Mater. Sci. Eng. 1107 (2021) 012234. https://doi.org/10.1088/1757-899X/1107/1/012234.

[6] A.V. Radhamani, H.C. Lau, S. Ramakrishna, Structural, mechanical and corrosion properties of CNT-304 stainless steel nanocomposites, Progress in Natural Science: Materials International 29 (2019) 595–602. https://doi.org/10.1016/j.pnsc.2019.09.007.

[7] L. Di Sarno, A. Majidian, G. Karagiannakis, The Effect of Atmospheric Corrosion on Steel Structures: A State-of-the-Art and Case-Study, Buildings 11 (2021) 571. https://doi.org/10.3390/buildings11120571.

[8] K. Pélissier, D. Thierry, Powder and High-Solid Coatings as Anticorrosive Solutions for Marine and Offshore Applications? A Review, Coatings 10 (2020) 916. https://doi.org/10.3390/coatings10100916.

[9] J. Telegdi, Multifunctional smart layers with self-cleaning, self-healing, and slow-release activities, in: Advances in Smart Coatings and Thin Films for Future Industrial and Biomedical Engineering Applications, Elsevier, 2020: pp. 457–486. https://doi.org/10.1016/B978-0-12-849870-5.00012-4.

[10] Lin Wang, SuNing Li, JiaJun Fu, Self-healing anti-corrosion coatings based on micron-nano containers with different structural morphologies, Elsvier 175 (n.d.) 107381. https://doi.org/10.1016/j.porgcoat.2022.107381.

[11] R.M. Parmar, Y.M. Parulekar, P. Kumar, G.R. Reddy, Seismic Analysis and Design of Steel Structures, in: G.R. Reddy, H.P. Muruva, A.K. Verma (Eds.), Textbook of Seismic Design, Springer Singapore, Singapore, 2019: pp. 235–306. https://doi.org/10.1007/978-981-13-3176-3_8.

[12] R.P. Edavan, R. Kopinski, Corrosion resistance of painted zinc alloy coated steels, Corrosion Science 51 (2009) 2429–2442. https://doi.org/10.1016/j.corsci.2009.06.028.

[13] A. Seth, W.J. Van Ooij, P. Puomi, Z. Yin, A. Ashirgade, S. Bafna, C. Shivane, Novel, one-step, chromate-free coatings containing anticorrosion pigments for metals—An overview and mechanistic study, Progress in Organic Coatings 58 (2007) 136–145. https://doi.org/10.1016/j.porgcoat.2006.08.030.

[14] Md.M. Uddin, M.H. Kabir, Md.A. Ali, Md.M. Hossain, M.U. Khandaker, S. Mandal, A. Arifutzzaman, D. Jana, Graphene-like emerging 2D materials: recent progress, challenges and future outlook, RSC Adv. 13 (2023) 33336–33375. https://doi.org/10.1039/D3RA04456D.

[15] S.S.A. Kumar, S. Bashir, K. Ramesh, S. Ramesh, New perspectives on Graphene/Graphene oxide based polymer nanocomposites for corrosion applications: The relevance of the Graphene/Polymer barrier coatings, Progress in Organic Coatings 154 (2021) 106215. https://doi.org/10.1016/j.porgcoat.2021.106215.

[16] R. Zhang, X. Yu, Q. Yang, G. Cui, Z. Li, The role of graphene in anti-corrosion coatings: A review, Construction and Building Materials 294 (2021) 123613. https://doi.org/10.1016/j.conbuildmat.2021.123613.

[17] F. Li, X. Jiang, J. Zhao, S. Zhang, Graphene oxide: A promising nanomaterial for energy and environmental applications, Nano Energy 16 (2015) 488–515. https://doi.org/10.1016/j.nanoen.2015.07.014.

[18] T. Zhang, T. Zhang, Y. He, Y. Wang, Y. Bi, Corrosion and aging of organic aviation coatings: A review, Chinese Journal of Aeronautics 36 (2023) 1–35. https://doi.org/10.1016/j.cja.2022.12.003.

[19] P. Joseph, S. Tretsiakova-McNally, Sustainable Non-Metallic Building Materials, Sustainability 2 (2010) 400–427. https://doi.org/10.3390/su2020400.

[20] E. McCafferty, Validation of corrosion rates measured by the Tafel extrapolation method, Corrosion Science 47 (2005) 3202–3215. https://doi.org/10.1016/j.corsci.2005.05.046.

[21] L.S. Ki, A.C. Ki, Z.V. Rtesy, L. Kiss, V. Ivanova, G. Raichevski, S. Vitkova, T. Marinova, Zn and Zn±Sn alloy coatings with and without chromate layers. Part I: Corrosion resistance and structural analysis, (n.d.).

[22] S.K. Shukla, A.K. Singh, M.A. Quraishi, Corrosion Inhibition and Adsorption Properties of N-Phenylhydrazine-1,2-Dicarbothioamide on Mild Steel in Hydrochloric Acid, International Journal of Electrochemical Science 6 (2011) 5779–5791. https://doi.org/10.1016/S1452-3981(23)18444-6.

[23] Y. Sasikumar, A.S. Adekunle, L.O. Olasunkanmi, I. Bahadur, R. Baskar, M.M. Kabanda, I.B. Obot, E.E. Ebenso, Experimental, quantum chemical and Monte Carlo simulation studies on the corrosion inhibition of some alkyl imidazolium ionic liquids containing tetrafluoroborate anion on mild steel in acidic medium, Journal of Molecular Liquids 211 (2015) 105–118. https://doi.org/10.1016/j.molliq.2015.06.052.

[24] Z. Salarvand, M. Amirnasr, M. Talebian, K. Raeissi, S. Meghdadi, Enhanced corrosion resistance of mild steel in 1M HCl solution by trace amount of 2-phenyl-benzothiazole derivatives: Experimental, quantum chemical calculations and molecular dynamics (MD) simulation studies, Corrosion Science 114 (2017) 133–145. https://doi.org/10.1016/j.corsci.2016.11.002.